Geomorphology 135 (2011) 129–142

Contents lists available at SciVerse ScienceDirect

Geomorphology

journal homepage: www.elsevier.com/locate/geomorph

Revisiting dirt cracking as a physical weathering process in warm deserts

Ronald I. Dorn *

School of Geographical Sciences and Urban Planning, Arizona State University, P.O. Box 875302, Tempe, AZ 85287-5302, United States

ARTICLE INFO

Article history:
Received 4 April 2011
Received in revised form 6 August 2011
Accepted 9 August 2011
Available online 17 August 2011

Keywords:
Calcrete
Desert geomorphology
Dust
Nanoscale
Physical weathering

ABSTRACT

A half century ago C.D. Ollier proposed that insolation-driven temperature changes expand and contract fill in fissures enough to widen cracks, a process that would permit progressively deeper penetration of fissure fills, that would in turn generate a positive feedback of greater and greater strain until desert boulders and bedrock shatters. Although desert physical weathering by "dirt cracking" has occasionally been cited, this hypothesized process remains without support from subsequent research. Here, field observations, electron microscopy, X-ray powder diffraction, particle-size analysis, and laboratory experiments shed new light on dirt cracking. Little clear evidence supports the original notion of expansive pressures from thermal fluctuations. However, mineralogical, high resolution transmission electron microscopy, back-scattered electron microscopy, and experimental evidence support two alternative processes of widening fractures: wetting and drying of fills inside fissures; and the precipitation and remobilization of calcium carbonate. A re-envisioned dirt-cracking wedging process starts with calcium carbonate precipitating in fissures less than 5 μm wide. First precipitation, and then ongoing dissolution of this laminar calcrete, opens enough space for dust to penetrate into these narrow fractures. Wetting of expansive clays in the fissure fill exerts enough pressure to widen and deepen the fissure, allowing the carbonate precipitation process to penetrate even deeper and allowing even more dust to move into a fracture. As the dust infiltrates, its texture changes from a chaotic mix of particles to an alignment of clays parallel to fissure sides. This parallel alignment could increase the efficiency of fill wedging. Ollier's concept of a positive feedback remains supported; each increment of fracture deepening and widening permits more, even deeper infiltration of laminar calcrete and dust. Field and electron microscope observations of rock spalling in the winter of 2010 are consistent with Ollier's hypothesis that dirt cracking is a common physical weathering process in deserts that splits rocks of all different sizes.

1. Introduction

Dirt cracking (Ollier, 1965), as originally envisioned, is a physical weathering process that splits desert boulders:

> "Evidence of dirt cracking is found in boulders with cracks that contain dirt but do not completely split the rock, and also in completely broken boulders with dirt between the several portions … Besides the large boulders there is evidence of dirt cracking on a smaller scale, breaking small boulders into angular fragments an inch or so across … The matrix of dirt consists of sand, clay, gravel … evidently carried into the crack and are not small fragments derived from the edges, for they are often rounded and iron stained … There may be some gypsum, but since this is not always present it is thought that the possibility of pressure due to crystal growth can be discounted … The postulated mechanism of dirt cracking is as follows: we will start with a boulder with slight cracks at the surface (whether insolation can cause initial cracking of a fresh boulder need not concern us here). Small particles of sand, silt or any other 'dirt' may lodge in the cracks. Expansion and contraction associated with temperature changes then act in two ways. First, differential expansion or contraction between the core and the surface of the boulder may cause cracks to open and close alternately. When a crack widens, dirt particles can enter deeper into the crevices. The particles then prevent the crack from closing to its former position, and so put the rock under strain. Second, the dirt particles themselves will be affected by expansion and contraction. On heating, a dirt particle will expand, forcing the crevice sides apart. On cooling, the particle will contract, and may fall deeper into the crack than it was originally. In the next expansion of the particle the boulder will be subjected to even greater strain. These two processes, it is believed, cause small initial cracks in a boulder to become wider. As they widen, larger and larger fragments can become lodged within them, enhancing the

* Tel.: + 1 480 965 7533; fax: + 1 480 965 8313.
E-mail address: ronald.dorn@asu.edu.

0169-555X/$ – see front matter © 2011 Elsevier B.V. All rights reserved.
doi:10.1016/j.geomorph.2011.08.010

effectiveness of the process, until eventually the boulder is completely shattered." (Ollier, 1965: 236–237)

The initial importance of dirt cracking to geomorphology included its role in the weathering and erosion of boulders, inselbergs and other desert landforms (Ollier, 1969, 1978).

In the half-century since Ollier's (1965) introduction, dirt-cracking has received only scant attention (Cooke, 1970; Mabbutt, 1977; Smith, 1988; Hall, 1989; Williams and Robinson, 1989; Kiernan, 1992; Clarke and Pain, 2004; Viles, 2005; Bourke and Viles, 2007; Chan et al., 2008; Smith, 2009; Jimoh, 2010). Repeating the basic idea of dirt cracking without mention of Ollier's (1965) paper has also occurred, for example, when the term 'fissuresol' was introduced to describe the mixture of mostly eolian dust with some weathered rock fragments that accumulate inside fractures in warm desert rocks in the Sonoran Desert (Villa et al., 1995) and create a weathering problem for petroglyph panels (Dorn et al., 2008). Another example of replication of concept includes this observation: "where permitted by climate, cracks in rocks can be havens not only for liquid water but also for fine-grained mineral dust and biological organisms. The presence of these actors may enhance the propagation of cracks that are able to grow large enough to admit either of these elements" (Moores et al., 2008: 479).

Dirt-cracking fines inside rock fissures are not the skeletal or embryonic soils found in rock-surface pits (Certini et al., 2002; Darmody et al., 2008). They are not the fracture fills found in saprolite and other in situ weathered rock (Thoma et al., 1992; Frazier and Graham, 2000). Instead, the mixture of eolian silt and rock fragments is found in fractures of all different orientations and sizes, but only in warm deserts where fractures accumulate dust (Goudie, 1978; Bullard and Livingston, 2009) — including the region studied here, Arizona and southwestern USA (Péwé et al., 1981; Brazel, 1989).

This paper's purpose rests in re-examining dirt-cracking processes. The starting point for Ollier's (1965: 237) hypothesis is the same as the starting point of this second iteration: "whether insolation [or other processes] can cause initial cracking of a fresh boulder [or bedrock] need not concern us here." While ongoing research has provided insight on how rock fractures initiate (Friedman, 1975; Engelder, 1987; Paradise, 2005; Viles, 2005; Warke, 2007; Moores et al., 2008; Adelsberger and Smith, 2009; Eppes et al., 2010; Smith et al., 2011), the way that cracks start in desert rocks is beyond the scope of this study because dirt cracking does not initiate fractures.

I hypothesize that the dirt-cracking process introduced in Australia is a common physical weathering process in warm and dusty drylands such as the Sonoran and Mojave deserts, and that dirt cracking proceeds through processes other than Ollier's (1965) original concept of insolation-driven expansion and contraction. After a presentation of study sites and methods, a section that combines results and discussion details findings from field observations, electron microscopy, and laboratory experiments. The paper ends by summarizing the revised dirt-cracking process.

2. Study sites

Five desert construction sites in southwestern USA provided a venue to study rock fractures formed in different rock types. Construction activities offer an opportunity to study fresh exposures of bedrock hundreds of meters long (e.g. Fig. 1). Four locations are in the Sonoran Desert, Arizona: gneiss of the Ma Ha Tuak Range (N 33.3511 W 112.0880) in the metamorphic core complex of South Mountain, Phoenix (Reynolds, 1985); early Proterozoic metavolcanic rocks (N 33.6822 W 111.8414) in the western McDowell Mountains (Richards et al., 2000), Scottsdale; early Proterozoic metasedimentary rocks (N 33.1361 W 111.6186) in the San Tan Mountains of central Arizona (Richards et al., 2000); and granodiorite in the Usery Mountains (N 33.4909 W 111.6702) of central Arizona (Richards et al., 2000). A fifth study site consists of basalt bedrock in the Mojave Desert, California, west of Barstow (N 34.8995 W 117.5129).

Ongoing rock spalling events offer an opportunity to better understand dirt-cracking processes. Thus, the southern side of the Guadalupe Range of South Mountain, central Arizona, served as the site to study the possible role of dirt cracking in rock spalling during the winter of 2010 (Fig. 2). Dome facets of this metamorphic core complex along the Desert Classic trail contain bedrock and tors that generated rock falls (Fig. 3) monitored between January 19th and April 10th, 2010.

3. Methods

3.1. Field methods

A mix of field and laboratory methods generated new insight into dirt cracking as a physical weathering process. In the first field study,

Fig. 1. Construction at the Las Sendas subdivision in the Usery Mountains of Mesa, Arizona, exposed hundreds of meters of granodiorite bedrock. These cross-sections of inselbergs made it possible to examine 300 fractures hosting fills of eolian dust and rock fragments. After opening fractures with a rock hammer, fines were washed away and data tabulated on the presence of orange iron films, the presence of an outer band of black rock varnish, and the presence of HCl-reacting laminar calcrete.

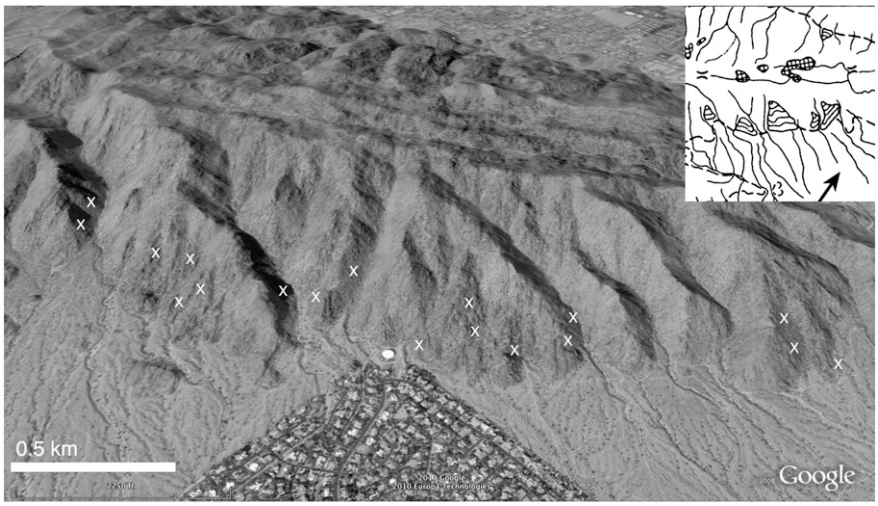

Fig. 2. The southeastern portion of Guadalupe Range of the South Mountain metamorphic core complex, Phoenix served as the field site for surveys of the role of dirt cracking associated with rock spalling. Newly identified wasting events are marked by X. The inset geomorphic map was modified from Pain (1985: 873), where dome faces are triangular shapes with idealized contours. On the inset map, hatched areas indicate summit areas of low relief; the lines indicate major drainages; and the arrow points North. The image follows permission guidelines for Google Earth. [http://www.google.com/permissions/geoguidelines.html].

Arizona State University students used rock hammers to pry open 300 fissures sampled randomly along ten 30-m long transects where rock outcrops were exposed at construction sites (e.g. Fig. 1). Additional samples of rocks with fractures were archived for laboratory study and for use in experiments. Students first identified whether the fills were composed of just eolian silt or a combination of eolian silt and

Fig. 3. Rock spalls that occurred during the El Nino Southern Oscillation event in the winter of 2010 (arrows identify source of the spalling) derive from steep bedrock slopes and tors on the southeast side of the Guadalupe Range of South Mountain, Phoenix, Arizona (see Fig. 2). The bright surfaces of recent spalls contrast with adjacent rocks covered with rock varnish and other dark rock coatings. Scale can be inferred from 3-m tall Paloverde (*Parkinsonia microphylla*) trees.

rock fragments that fell into the crevice. Then, students washed away eolian fines and weathered rock inside fractures with water. For each fissure, students observed rock coatings on the sides of the opened fissure documenting: the presence or absence of orange iron film coatings; the presence or absence of a cm-scale black band of rock varnish on the outermost portions of a fissure; and the presence or absence of laminar calcrete that reacts strongly with HCl.

A second field study involved observations of rock spalling events and their possible connection to dirt cracking. The 2009–2010 El Niño Southern Oscillation (ENSO) produced a wet winter in central Arizona. After direct observation of a rock fall on January 19th, 2010, dome facets and other steep bedrock surfaces of the South Mountain metamorphic core complex, Phoenix (Pain, 1985), were monitored for rock spalls along the Desert Classic trail of South Mountain Park, Phoenix (Fig. 3). Bedrock surfaces observable from the trail were surveyed at least three times a week for any changes. Upon identification of a possible new spall, Maricopa County Tax Assessor's aerial photography (Maricopa-County, 2010) was examined at scales of 1:400 from November/December 2008 and November/December 2009; 18 spalling events identified in field surveys were confirmed as not present in the aerial photography. Because surveying was not daily, mass wasting events could only be constrained in time as being between surveys; results were tabulated and compared with precipitation recorded at an automated rain gauge less than 2 km distant. Opened bedrock surfaces at all spalls were examined in the field for evidence as to whether dirt cracking might have played a role in the failure, as indicated by the presence of exposed fissure fills and laminar calcrete on spalled surfaces and within newly exposed bedrock fractures widened by spalling.

In addition, an assortment of fissures from sites scattered across the Mojave, Great Basin, and Sonoran Deserts provided samples for the study of laminar calcrete and dust by backscattered electron microscopy. These sites include: Burnt Mountain, Sonoran Desert, AZ; Joshua Tree, Mojave Desert, CA.; Black Mountains, Death Valley, CA: McDowell Mountains, Sonoran Desert, AZ; Cougar Buttes, Mojave Desert, CA; and Florence Junction, Sonoran Desert, Az.

3.2. Laboratory studies

High Resolution Transmission Electron Microscopy (HRTEM), backscattered electron microscopy (BSE) and energy dispersive X-ray analyses (EDS), and wavelength dispersive (WDS) electron microprobe analyzed samples of rocks with fractures collected from construction sites. In addition, opened bedrock surfaces at South Mountain, Phoenix, were sampled for fill material, and samples from the walls of these fissures were collected for study using these electron microscope methods.

X-ray powder diffraction (XRD) was used to analyze the mineralogy of samples collected from fissure fills at each of the five construction sites. A Beckman Coulter laser particle size analyzer measured the percent sand, silt and clay for particles less than 2 mm in diameter from these fissure fills.

3.3. Experiments on dirt cracking processes

A laboratory experiment assessed Ollier's (1965) hypothesis that insolation-driven temperature changes cause expansion and contraction of fissure fills that results in the gradual opening of fractures. Two additional experiments assessed an alternative hypothesis that wetting and drying of fill inside a fissure apply enough expansive pressure to widen fractures, and then "[w]hen a crack widens, dirt particles can enter deeper into the crevices. The particles then prevent the crack from closing to its former position, and so put the rock under strain" (Ollier, 1965: 237).

The idea behind these experiments rests in subjecting fissure fills to temperature or moisture changes and then measuring any expansion that occurs. An inherent difficulty is not knowing if a fracture fill truly existed inside each of the collected samples before each experiment, because opening up a fracture to check for the presence of fill material destroys the integrity of a sample for an experiment. While hand lens examination of rock chips identified the presence of one or more cracks in each sample and the apparent presence of dust inside these cracks, the experiment had to proceed with the operating assumption that fissure fills actually existed in the samples. The step of determining the presence and width of any fill material could only be accomplished after the experiment had terminated.

The samples of rock fragments were collected from a construction site at the base of the Ma Ha Tuak range, Arizona that exposed gneiss bedrock. For each experiment, fifty gneiss samples with volumes ranging from 200 to 2000 cm^3 were pried gently from the bedrock.

The first experiment involved a single wetting and heating event for 50 gneiss rock chips. Each gneiss sample was placed in a mold that allowed a side of the rock chip to be covered in epoxy, where the chip was oriented in a way that unopened fractures were parallel to the flat epoxy surface. In essence, the epoxy just served as an easy way to handle the rock chips so that the chips could be exposed to experimental conditions and to facilitate measurements with a Vernier caliper. Unopened fractures were exposed to the atmosphere on all sides. The epoxy allowed clasts to be oriented such that fractures could be placed under a small rainfall simulator with raindrop sizes of about 5 mm.

Rainfall collected from a Sonoran Desert thunderstorm was then distributed on the clasts in one event at a rate equivalent to 25.4 mm of precipitation over 10 min; this intensity is not unusual in Sonoran Desert summer thunderstorm downbursts. Table 1 presents the elemental composition of this rainfall, as measured by Inductively Coupled Plasma – Mass Spectrometry (ICP-MS). Then, after wetting, a Vernier caliper measured any expansion that might have occurred from this simulated wetting and heating event, to the nearest 0.05 mm.

After wetting, samples were heated in an oven at 90 °C for 48 h. This baking process was not meant to simulate any real-world condition. The baking was to drive off water prior to sectioning the samples. Then, a Vernier caliper remeasured widths to assess if any change expansion occurred.

A second experiment involved ten wetting events for another 50 gneiss samples with unopened fractures. This experiment used the same rock chip preparation and wetting process. However, heating in an oven did not take place. Samples were allowed to air dry at room temperature for 7 days, before being subject to a repeated wetting event of 24.5 mm of precipitation. After the tenth cycle of wetting and

Table 1
ICP-MS analyses of Sonoran Desert rainwater used in the experiment on fissuresol expansion.

Element	Detection range	Concentration (μm/l)
Al	50–10,000	590
Ba	0.01–1000	12
Ca	200–10,000	1561
Cd	0.1–1000	0.6
Cr	1–1000	2
Cu	0.3–1000	25
Fe	20–10,000	162
K	60–10,000	84
Mg	4–10,000	266
Mn	0.1–1000	18
Na	300–10,000	410
Ni	0.5–1000	1.8
Pb	0.2–1000	94
Sb	0.1–1000	0.2
Tl	0.04–1000	11
V	1–1000	6
Zn	2–1000	17

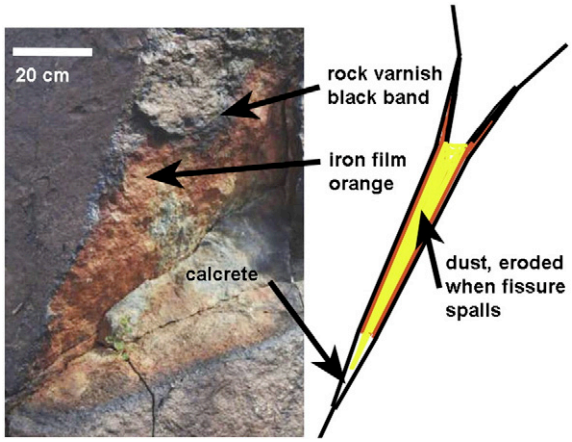

Fig. 4. This fissure once hosted eolian dust and some weathered rock fragments that were washed away prior to photography. The innermost side of the opened fissure is coated with laminar calcrete. The outer few centimeters are coated by a ring of black rock varnish. The remainder of the fracture side is covered by an orange iron film.

air drying, a Vernier caliper measured any expansion related to these simulated wetting event, to the nearest 0.05 mm.

A third experiment involved ten heating and cooling events for another 50 gneiss samples with unopened fractures. Wetting did not take place in this experiment. An oven heated samples at 80 °C for 8 h and then samples cooled at room temperature for 16 h, before being subject to a repeated heating event. Selection of the temperature of 80 °C is based on infrared thermometer (IRT) measurements of naturally exposed clasts in the Ma Ha Tuak Range in June, where IRT readings of 80 °C occur on rock surfaces during the hottest days in Phoenix, Arizona. After the tenth cycle of heating and cooling, a Vernier caliper measured any expansion related to these simulated heating events, to the nearest 0.05 mm.

After each experiment concluded, samples were completely entombed in epoxy to facilitate the creation of a cross-section. Cross-sections were used to measure thicknesses of any fracture fills that may have been inside the fractures. Fill thicknesses were measured with the aid of a binocular microscope at 45×. Some of the samples had more than one fracture. Thus, where multiple fills occurred in a sample, their thicknesses were summed for comparison with any expansion that might have occurred.

Table 2
Abundance of different types of rock coatings found on the sides of 300 fractures that were infilled with fissuresols, tabulated after fracture sides were washed with distilled water.

	Ma Ha Tuak Range, South Mountain, Phoenix, AZ.	McDowell Mountains, Scottsdale, AZ.	San Tan Mountains, Queen Creek, AZ.	Usery Mountains, Mesa, AZ.	West of Barstow, Mojave Desert, CA.
Lithology	Gneiss	Metavolcanic	Metasedimentary	Granodiorite	Basalt
Iron film	100%	100%	100%	100%	100%
Black varnish band	78%	73%	81%	84%	77%
Laminar calcrete	32%	24%	18%	30%	27%

Table 3
Particle size percentages of the less than 2 mm size fraction, and mineral components of clay (<2 μm) size fraction from fissuresol fills. XRD-measured mineral components are listed in order of decreasing abundance as estimated from X-ray diffraction patterns where +++ is >50%, ++ is 10–50%, and + is <10%.

	Ma Ha Tuak Range, South Mountain Phoenix, AZ.	McDowell Mountains, Scottsdale, AZ.	San Tan Mountains, Queen Creek, AZ.	Usery Mountains, Mesa, AZ.	West of Barstow, Mojave Desert, CA.
Lithology	Gneiss	Metavolcanic	Metasedimentary	Granodiorite	Basalt
Percent sand	8.20	14.52	6.97	10.36	13.46
Percent silt	77.90	67.71	73.58	70.97	58.50
Percent clay	13.90	17.77	19.45	18.67	28.04
Feldspar		+	+		
Kaolin	+	++	++	++	++
Mica	++		++	+	+
Palygorskite			+		
Quartz		+	++		+
Smectite	+++	++	+++	+++	+++
Vermiculite		++			

4. Results and discussion

4.1. Field Observations

Ollier (1965) presented photographs of fractured boulders with fines found inside opened crevices. Ollier's basic observations have been replicated in different deserts and at scales from cm-sized fractures to m-long crevices (Coudé-Gaussen et al., 1984; Villa et al., 1995; Dorn et al., 2008; Moores et al., 2008). Observations at the five construction sites and spalling study site reveal that fissure fills also found fills in fractures that have all different orientations; they can be vertical, horizontal or oblique. As Ollier (1965) noted, the scales of fissure fills vary tremendously. The fills can extend into fissures

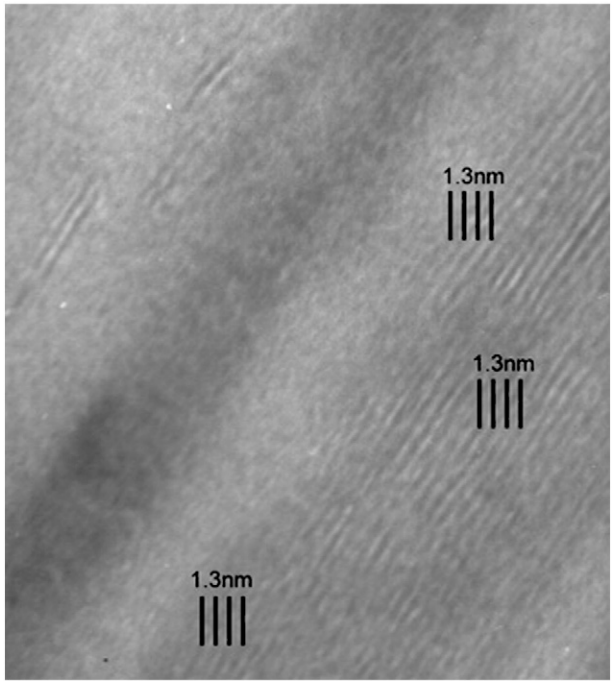

Fig. 5. HRTEM lattice fringe image of fissure fill from the Ma Ha Tuak Range of South Mountain, Phoenix. The image shows smectite fringes with spacing at about 1.3 nm. Diffuseness is due to variable layer thicknesses and variable layer orientation.

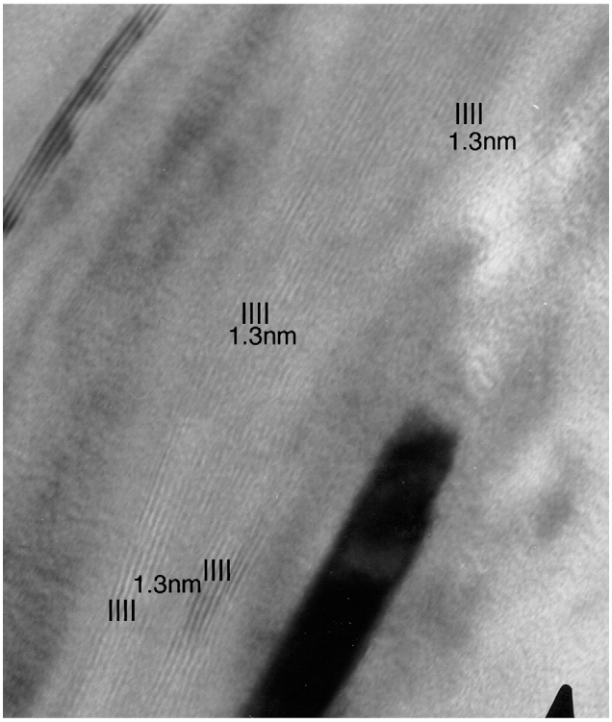

Fig. 6. HRTEM lattice fringe image of fissure fill from the McDowell Mountains, Scottsdale, Arizona. The image shows smectite fringes with spacing at about 1.3 nm. Diffuseness is due to variable layer thicknesses and variable layer orientation. Opaque shapes are particularly thick minerals.

several meters, as seen in recently made road cuts, but typical penetrations are less than a meter.

Observations of crevices in the Sonoran, Great Basin, Mojave, and Chihuahua Deserts in North America that were opened physically with the assistance of a rock hammer reveal that the fill inside fissures always includes eolian silt and also includes angular rock fragments that fell into a fissure 78% of the time. These observations also reveal a repeated pattern in the zonation of rock coatings seen in the walls of the fissure.

Once a fissure is pried open and the fissure fill is washed away, both sides of the crevice are coated with a colorful and distinctive pattern of rock coatings (Fig. 4). Laminar calcrete, orange iron film, and black rock varnish occur in a regular sequence. Laminar calcrete occurs in the innermost portions of a fracture. Black rock varnish rings the outermost portion of a crevice. Crevice side walls between the calcrete and black ring of varnish are coated by an orange iron film. Both laminar calcrete and orange iron films are found in contact with fissure fines, but the fines are not in contact with the narrow band of black varnish.

Field observations of 300 dust-filled fractures from five different construction sites reveal insights into the relationship between the presence of a fissure fill and the occurrence of rock coatings on fissure walls. Table 2 tabulates these observations; after washing away fills with distilled water, iron films were noted on the fracture sides in contact with all 1500 fills. About three-quarters of the fracture sides had a black band of rock varnish along the outer centimeters of a fissure, and laminar calcrete was tabulated to occur on 18% to 32% of the fracture sides.

4.2. Textural and mineralogical observations of fracture fills

For the less than 2 mm size fraction, silt is the dominant particle size (Table 3) — ranging from 58% to 78%. The abundance of silt is consistent with an abundance of summer dust storms (Brazel, 1989; Marcus and Brazel, 1992). Percent clay ranges from 14% to 28% of the measured fills.

X-ray diffraction (XRD) analyses of the clay-sized fraction from one fissure collected from each of the five sites indicates that smectite is the most common mineral, with kaolin, feldspar, mica, and quartz observed in more than one fissure (Table 3). Although Ollier (1965) identified some gypsum in fracture fills in Australia, no detectable gypsum occurred in these samples. However, small quantities of iron nitrate, barium oxide, and sodium chloride were observed, but in concentrations of far less than 1%.

High resolution transmission electron microscopy (HRTEM) observations carried out on samples from each site offer a comparison with XRD findings. HRTEM observations confirm that smectite is common in the five fissure fills examined — for example at South Mountain, Phoenix, collected from the Ma Ha Tuak Range (Fig. 5) and in a sample collected from a McDowell Mountains, Scottsdale, fissure (Fig. 6).

The expansive clay content of fissure fills would be consistent with a dirt-cracking process that involves expansion and contraction from wetting and drying. Then, after each expansion and contraction event, fissure-fill particles could penetrate deeper into a fracture.

4.3. Electron microscopy of rock coatings on fracture walls

The orange iron films and black rock varnish bands found on fissure side (Fig. 4; Table 2) do not appear to play a role in dirt cracking. They simply form on fissure walls in response to this

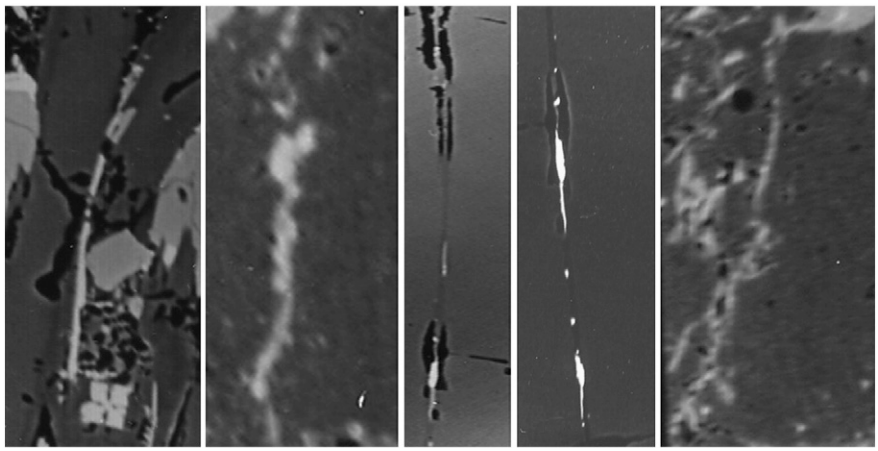

Fig. 7. Back-scattered electron micrographs of laminar calcrete (bright lines) formed in narrow fissures. Energy dispersive X-ray analyses reveal that calcium and carbon dominates the linear light-colored material. The images from left to right derive from: Burnt Mountain, Sonoran Desert, Az; Joshua Tree, Mojave Desert, CA.; Black Mountains, Death Valley, CA: McDowell Mountains, Sonoran Desert, AZ; and Cougar Buttes, Mojave Desert, CA. Widths of calcrete infills are approximately 2 μm, 4 μm 2 μm, 2 μm and 3 μm from left to right.

landscape geochemical setting of alkaline dust in contact with rock (Dorn, 2009). However, the precipitation of laminar calcrete found inside opened fissures appears to play a role in dirt cracking.

While there exists a substantial literature on laminar calcrete in pedogenic contexts (Chitale, 1986; Wright, 1989), the literature on laminar calcrete found inside desert rock fractures is more limited. Observations of calcrete vein precipitation reveal the power to split grains of quartz sand (Rockrock, 1925) and terrace gravels (Young, 1964). Mechanical excavations of Navajo Sandstone near Hurricane, Utah, reveal the presence of calcrete-filled bedding-plane fractures and calcrete-filled vertical joint fractures, where the calcrete precipitation process appears to play a role in bedrock fracturing (Heilweil and Solomon, 2004). Isotope studies of calcite precipitation within basalt rock fractures in different Arizona volcanic fields reveals a role for the removal of ^{12}C by photosynthetic communities such as lichens during evaporation on rock surfaces, and the removal of ^{12}C alters the stable carbon isotope composition of the intra-basalt precipitated calcite (Knauth et al., 2003). Yucca Mountain, Nevada, studies of calcrete formed in bedrock fractures reveal a variety of processes including dissolution of rock material, a role for bacteria in cycling the calcium trapped in oxalates into calcite, as well as ongoing calcite dissolution and then reprecipitation (Vaniman and Whelan, 1994).

Dust in Arizona and elsewhere in the desert southwestern United States contains an abundant source of carbonate (Péwé et al., 1981; Schlesinger, 1985). The hypothesis proposed here is that infiltrating water dissolves carbonate from dust that moved into the narrowest and deepest section of a crevice. The carbonate then precipitates in these narrow fractures, as shown in Fig. 7; these calcrete-filled fissures came from about 10 cm deep into sampled fractures. These BSE images reveal calcrete only a few microns in width. In a few fractures, the calcrete appears to be dissolving, leaving behind some pore space. In other samples, calcrete completely fills a fracture — revealing a possibility that laminate calcrete might also be able to seal cracks (cf. Heilweil and Solomon, 2004). It appears as though the calcrete is unstable, undergoing both mobilization and reprecipitation of calcrete (cf. Vaniman and Whelan, 1994). While lichens appear to influence pedogenic calcrete formation (Klappa, 1979), and isotopic evidence suggests lichens influence carbon fractionation in laminar

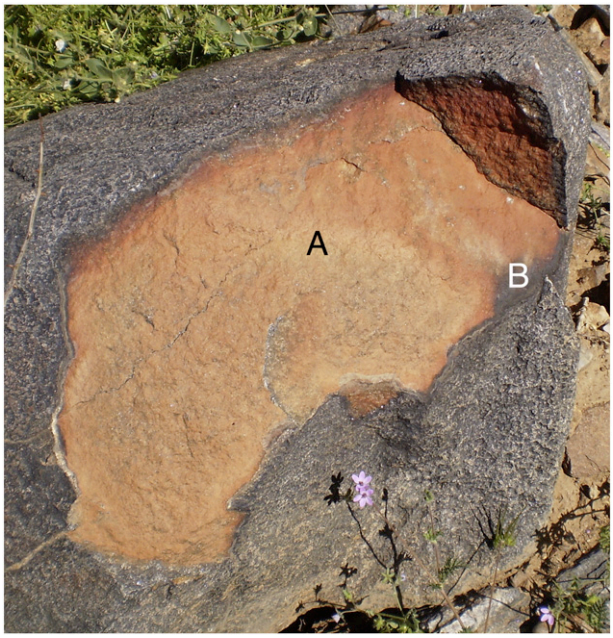

Fig. 9. A fissure was mechanically pried open and samples were removed by a rock hammer for thin sectioning and wavelength dispersive electron microprobe analyses. Letter A (in the middle of the orange-colored iron film) is the location of the section in Fig. 10A. Letter B (in the narrow band of black varnish along the rim of the opened fissuresol) is the location of the section in Fig. 10B. The 1.3 cm diameter of the *Eriastrum diffusum* wildflower in the lower middle of the image provides scale.

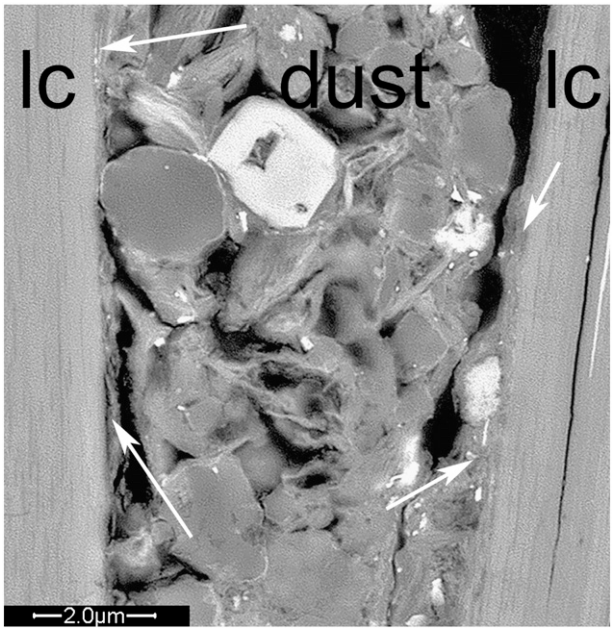

Fig. 8. Back-scattered image of a fissure fill where laminar calcrete (on the sides) first precipitated and then dissolved enough to allow dust to infiltrate into the fracture. As is typical of the first penetration of dust, the particles are arrayed in a chaotic mix of silt and clay-sized particles. The 'lc' annotation identifies the laminar calcrete; the word 'dust' indicates the dust infill; the black arrow indicates a location where the laminar calcrete may be undergoing dissolution; and the white arrows identifies loci where the calcrete appears to be precipitating. This sample came from a fractured boulder near Florence Junction, Sonoran Desert, AZ.

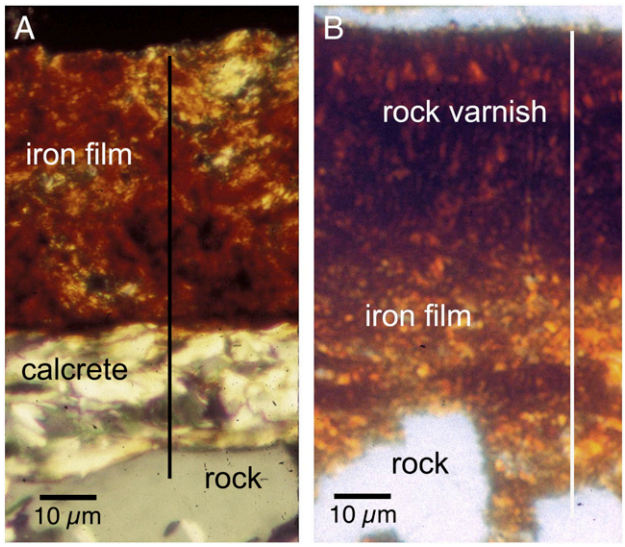

Fig. 10. Optical thin sections show superimposition of different rock coatings formed on the sides of a fissure. Images A and B correspond to collection locales indicated in Fig. 9. Lines indicate the location of electron microprobe transects. A. Optical thin section showing calcrete that coats quartz composing a fissure sidewall. Then, the fissure opened wide enough accumulate dust and weathered fragments. This dust fostered the formation of the orange iron film on top of the calcrete. B. Optical thin section first showing the formation of orange iron film. Then, the rock fracture opened wide enough for rainwater to wash the accumulated dust away from the rock surface. This allowed the formation of black manganese-rich rock varnish.

Table 4
Wavelength dispersive electron microprobe analyses of an iron film superimposed on laminar calcrete lining a fissuresol from South Mountain, Phoenix, with the location of the sample identified in Fig. 9 with the letter A. The analyses were measured along the line in Fig. 10A. Totals are less than 100% due to porosity, water, and trace and rare elements not analyzed.

Depth (μm)	NaO	MgO	Al_2O_3	SiO_2	P_2O_5	$S0_3$	K_2O	CaO	TiO_2	MnO	Fe_2O_3	Total	Material
5	bld	2.06	11.40	35.98	0.76	0.22	2.24	0.78	0.49	1.97	19.29	73.13	Fe film
10	bld	1.82	12.20	36.89	0.54	0.27	0.55	0.91	0.81	1.84	20.47	74.48	Fe film
15	0.09	3.07	16.91	35.93	0.53	0.16	0.91	0.48	0.65	1.52	17.47	74.56	Fe film
20	0.06	2.24	15.17	28.63	0.12	0.21	1.63	0.93	0.48	1.99	19.91	69.07	Fe film
25	0.07	2.37	19.68	30.79	0.31	0.26	1.28	1.85	0.35	0.86	16.49	71.87	Fe film
30	0.11	2.16	14.21	29.38	0.67	0.28	1.48	0.89	0.47	1.45	17.35	66.18	Fe film
35	bld	2.33	15.02	30.56	0.28	0.21	3.45	1.72	0.90	3.93	24.26	80.33	Fe film
40	bld	1.65	16.73	31.76	0.25	0.31	0.73	5.43	0.67	4.73	19.31	79.92	Fe film
45	0.07	bld	0.71	3.39	bld	bld	0.19	61.84	bld	bld	0.77	66.90	Calcrete
50	0.05	bld	0.35	8.22	bld	bld	0.14	77.23	bld	bld	2.18	88.12	Calcrete
55	bld	bld	0.17	98.37	bld	bld	bld	Bld	0.16	bld	0.24	98.94	Quartz

calcretes (Knauth et al., 2003), electron microscopic observations carried out here did not reveal any direct visual for a microbial role.

Portions of fissures closer to the surface reveal separation of laminar calcrete and subsequent infilling with dust (Fig. 8). Submicron wavy textures in the separated laminar calcrete suggest that dissolution features inside the calcrete may have generated weaknesses that were exploited as a fissure widens.

There are different possible ways that laminar calcrete might relate to dirt cracking as a physical weathering process. One is that the laminar calcrete is adventitious — that it formed long before the crevice was exposed to the subaerial environment. A second possibility is that the laminar calcrete is the first step in dirt cracking, as hypothesized here — that water carries dissolved carbonate into fissures and its precipitation plays a role in the initial widening of the fracture. A third possible connection is that carbonate enhances crack widening through first precipitation of the calcrete in a fracture; further wetting events dissolve some, but not all, of the calcrete that is later replaced by dust penetrating deeper into the fissure. A fourth possibility is a combination — that some calcrete could be adventitious, while newly formed calcrete could represent an initial wedging process that starts to open the fissure wide enough to permit the penetration of dust.

One of the reasons why calcrete was not observed as frequently as the other rock coatings in field observations (Table 2) could be connected with the sequence of coating formation in a rock fracture. A working hypothesis is that calcrete forms first deep inside a fracture. Then, partial dissolution of calcrete opens the fissure wide enough to allow infiltrating dust to penetrate (Fig. 8). However, not all of the calcrete remobilizes deeper into the fracture. Some remains. The calcrete that remains on the wall of a fissure is coated by dust. Alkaline dust promotes the formation of orange iron films that cover some of the laminar calcrete. This sequence can be seen in Figs. 9 and 10A. Thus, calcrete can occur underneath orange iron films in cross-sections, and these are not seen in the field.

Wavelength dispersive electron microprobe analyses reveal that the orange iron film from the Ma Ha Tuak Range of South Mountain, Phoenix (Figs. 9, 10A), is dominated by the aluminum and silicon of clay minerals (Table 4). This particular iron film contains about 20% Fe-oxide, an amount that is about two to four times normally found for iron films in on fracture walls (Dorn, 1998). Microprobe analyses of a band of black rock varnish (Figs. 9, 10B) from this same fissure indicates major and minor elemental abundances similar to other rock varnishes in the southwestern USA (Dorn, 1988) with manganese and iron in equal proportions and totaling about 30% by oxide weight (Table 5).

Optical thin sections and electron microprobe analyses reveal a distinct microstratigraphy in fissure-wall rock coatings. Calcrete occurs underneath orange iron film in the innermost portion of the pried-open crevice (Letter A in Figs. 9, 10; and Table 4). Thus, the orange iron film that is so ubiquitous (Table 2) can mask the presence of laminar calcrete that formed first in fissures. Then, orange iron film occurs underneath black varnish in the outermost portion of the pried-open crevice (Letter B in Figs. 9, 10; and Table 5). Manganese-rich rock varnish starts to form only when the fissure opens wide enough for penetrating water to wash away fines.

4.4. Observations of new spalling events

Dome facets and other steep bedrock surfaces of South Mountain, Phoenix (Pain, 1985), were monitored for rock spalls along the Desert Classic trail of South Mountain Park, Phoenix (Figs. 2, 3). One rock spall was observed directly and seventeen were tabulated to have taken place in the winter of 2010 and early spring at South Mountain, Phoenix

Table 5
Wavelength dispersive electron microprobe analyses of a band of black rock varnish superimposed on an iron film that coats the side of a fissuresol from South Mountain, Phoenix, with the sample collection locale identified in Fig. 9 with the letter B. The analyses were measured along the line in Fig. 10B. Totals are less than 100% due to porosity, water, and trace and rare elements not analyzed.

Depth (μm)	NaO	MgO	Al_2O_3	SiO_2	P_2O_5	$S0_3$	K_2O	CaO	TiO_2	MnO	Fe_2O_3	Total	Material
5	0.44	1.00	14.44	22.09	2.55	0.15	3.74	2.07	1.22	19.23	18.73	84.22	Black band
10	0.25	0.87	16.20	19.31	2.34	0.12	4.70	1.83	0.56	16.44	16.76	78.26	Black band
15	0.28	1.14	15.49	23.94	2.26	0.07	3.46	2.38	1.35	16.05	14.41	79.41	Black band
20	0.52	1.64	17.78	26.08	1.79	0.09	2.14	2.20	1.38	13.16	15.13	79.75	Black band
25	0.50	1.57	16.96	19.09	2.12	0.11	3.42	2.37	0.74	17.94	17.60	80.35	Black band
30	0.26	0.92	18.96	22.73	2.06	0.20	3.31	2.08	1.24	7.04	16.62	74.24	Black band
35	0.45	3.73	19.33	21.59	1.76	0.26	4.22	2.35	0.84	13.54	15.44	79.33	Black band
40	0.07	2.81	18.22	33.08	0.72	0.27	2.07	0.73	0.47	5.23	19.81	80.60	Fe film
45	0.05	3.46	12.82	30.07	0.59	0.47	2.19	0.79	0.59	3.56	17.40	68.48	Fe film
50	bld	1.71	13.96	37.83	0.88	0.12	1.61	0.79	0.41	3.31	17.14	76.05	Fe film
55	0.06	2.41	14.59	36.36	0.98	0.26	1.25	0.91	0.5	2.03	21.11	77.99	Fe film
60	0.08	2.06	20.07	30.05	0.86	0.38	3.87	0.93	0.44	2.51	20.50	79.61	Fe film
65	bld	3.03	12.95	28.21	0.44	0.25	3.81	0.96	0.61	3.54	21.79	72.56	Fe film

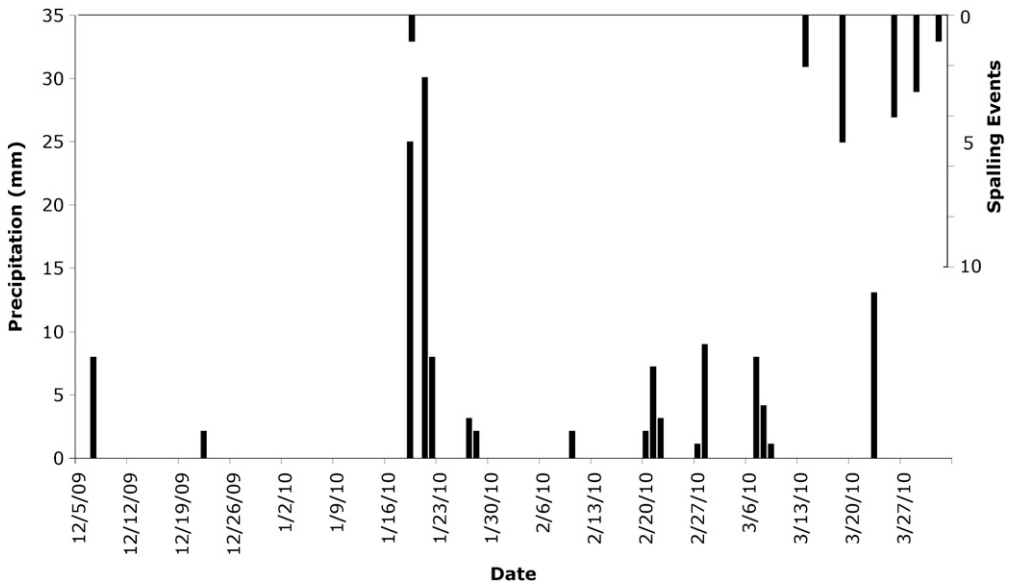

Fig. 11. Timing of South Mountain, Phoenix, spalls in relation to precipitation events. The timing of spalls plots on the middle day between field observations.

(Fig. 11). Figs. 3, 12 and 13 exemplify these new spalls, and all showed evidence of fills inside the fractures. Similarly, all newly examined spall breaks occurred where laminar calcrete had precipitated in fissures. No earthquakes, insect activity, or other potential process was in evidence as having contributed to the spalls. While spalls are close to a major multi-use trail, people rarely climb on these steep slopes. While animal activities are known to transport rock fragments in drylands (Evenari et al., 1982; Govers and Poesen, 1998), the particular positions of many of the spalls make it highly unlikely that javelinas, coyotes, rabbits, or other animals common at South Mountain would have set off the rock falls.

Tabulating mass wasting events on a histogram of precipitation reveals that most of the observed rock spalls did not occur during or immediately after rainfall. The timing of spalling in relationship to precipitation events (Fig. 11) suggests that water lubrication or expansion of fissure fills from wetting was not the obvious cause of failure, because most of the observed spalling events took place in mid to late March, after daytime high temperatures had risen to above 20 °C and after considerable drying had taken place.

Wetting and drying cycles of clays exert enough physical stress to weather rock material, even in drylands (Griggs, 1936; Smith, 1994; Gökceogu et al., 2000). Well-known expansion properties of smectite clays offer a possible explanation for opening desert fissures (Haward et al., 1969; Kittrick, 1969; Watanabe and Sato, 1988). In order to better understand the role of drying after wetting in dirt cracking of desert rocks, samples collected from the point of spalling were epoxied in order to preserve in situ relationships (Figs. 12 and 13). The samples were examined with BSE and HRTEM. BSE, however, did not prove to be an effective way of studying these failure spots. This is because the level of resolution available was insufficient to determine the mineralogy of clays involved.

A sample collected from the detachment fracture, but still a part of the bedrock (arrow in Fig. 12) shows that the fracture that failed extended into the fill. The fill appears to have developed a new

Fig. 12. Consequence of a spalling event observed directly on January 19th, 2010. Two rectangular solids broke from the overhang — where the failed fractures were coated with laminar calcrete and iron film. Then, a 3 m by 1 m piece of the overhand broke off, dropping 2 m and sliding another meter; the failed surface hosted laminar calcrete, iron film, and the narrow band of black varnish. Samples were collected at the initial failure surface (see arrow).

Fig. 13. This spall took place between 5 pm January 25th and 5 pm January 27th, 2010. A 2.5-m cube-shaped block first separated from bedrock and settled in a position in the lower left portion of the image. A sample was collected at the arrow, from within a partially opened fracture.

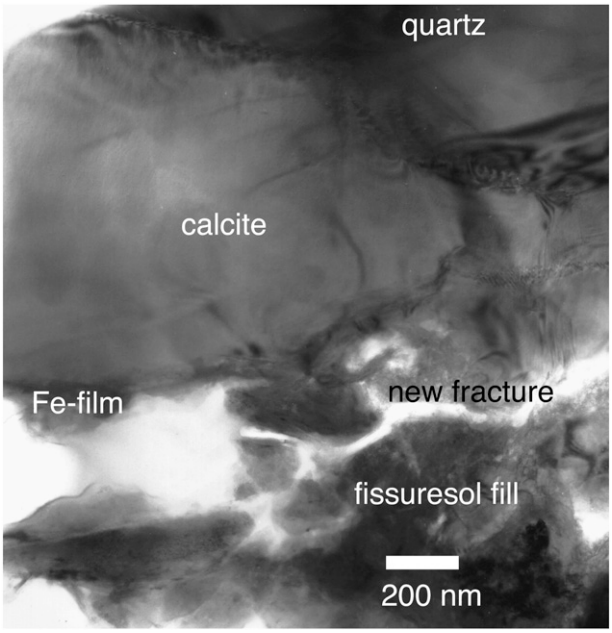

Fig. 14. HRTEM image acquired arrow in Fig. 12. Quartz at the top is the rock side of the fissure. Calcite (laminar calcrete) deposited on top of the quartz, followed by an iron film and then by fill deposited in the fissure. Then, a fracture formed inside the fissure fill. EDS analyses determined the composition of these materials.

internal fracture within the fill (Fig. 14), perhaps the result of desiccation and contraction of the fill.

At another spall location, a meter-sized fragment had not yet separated from the bedrock. A sample collected from inside that partially-separated fracture (arrow in Fig. 13) does not show calcrete next to the fissure sides, but the presence of expansive clay minerals (Fig. 15). The orientation of the clay minerals parallel to a fracture side would make swelling with wetting and shrinking with drying more effective in applying pressure than randomly oriented clays.

Another sample collected just 2 cm in from the outer edge of the partially separated fracture (Fig. 13) reveals a very different texture. Fissuresol fill closer to opening of the fracture appears much more disorganized (Fig. 16). Oval-shaped fragments of layered phyllosilicate minerals do not appear to be oriented parallel to fracture side walls.

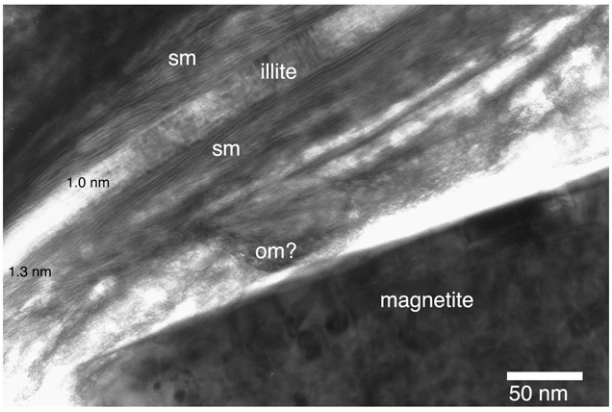

Fig. 15. HRTEM image of the location of a partially-opened fracture. The sample was collected from the arrow in Fig. 13. The side of the fracture in granodiorite is indicated by magnetite (EDS determined composition). Next to the magnetite is unknown material with a granular texture typical of decaying organic matter (om?). The nature of the clays in the fissuresol infill deep into this fissure shows an orientation parallel to the layered texture. This image is typical in that there is a mixture of illite and smectite (sm). The illite has a spacing of 1.0 nm. The darker portions of the smectite are too thick for spacing measurement, but the thinner portions show spacings of 1.3 nm.

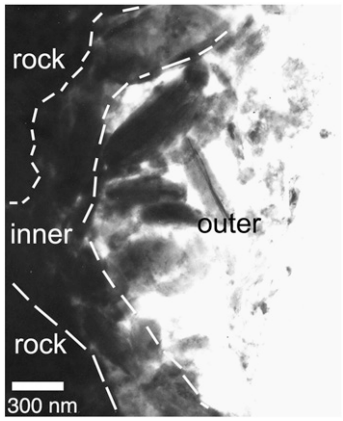

Fig. 16. HRTEM image of a partially-opened fracture collected from inside the partially opened fissure in Fig. 13, but just 2 cm from the fissure's outer edge. The fill in the fissure is mostly disorganized particles of dust, as revealed in the "outer" portion of this image. However, the dust closest to the rock surface does appear to be undergoing some reorganization and repacking in the closest half-micron to the rock on the fissure side.

One hypothesis is that the clay minerals inside fissuresols have similarities to clay minerals in more traditional cumulic soils. Cumulic dust that first settles into a fissure is poorly organized (Figs. 8, 16). Then, a process not unlike illuviation orients the clay mineral phyllosilicate structure parallel with the movement of water into the fissure (Fig. 15).

In the end, it is impossible to know for sure that rocks spalled at South Mountain, Phoenix, due to dirt cracking gradually widening a fracture to the point where failure occurred. Generally, rockfall associated with a critical meteorological event such as storms would occur within hours to days. Instead, rock fatique by widening of pre-existing fractures is a reasonable interpretation. A progressive decrease in rock material strength could have been achieved through dirt cracking. Laminar calcrete lined these fractures; fines occurred each fracture; expansive clays were in these fills; as the clays migrated deeper into the fractures, they aligned parallel to the fracture sides; and fracturing propogated into the expansive clays themselves. A reasonable possibility is that dirt cracking played a role in the observed spalling events, and perhaps a key role.

4.5. Experiments

In contrast to the insolation hypothesis offered by Ollier (1965), well-known expansion properties of smectite clays offer a possible explanation for opening desert fissures by dirt cracking (Haward et al., 1969; Kittrick, 1969; Watanabe and Sato, 1988). To understand the comparative roles of these alternatives, three simple experiments, each conducted on 50 gneiss rock chips, evaluated whether wetting and temperature changes could cause fissure fills to exert expansive pressures on fracture side walls. One experiment simulated 25.4 mm of precipitation followed by oven drying and measuring the maximum amount of expansion with a caliper. Many fractures did not widen at all with wetting, and the maximum amount of expansion was only 0.55 mm, where the caliper's reading has an uncertainty of ± 0.05 mm (Fig. 17).

Another experiment simulated ten wetting events of 25.4 mm of precipitation, each followed by 7 days of air drying at room temperature. Results reveal fewer fractures exhibiting no expansive pressure and a slightly enhanced relationship between the thickness of a fissure fill and the maximum measured expansion (Fig. 18).

Although these measured effects are small, the slight tendency for more expansion to occur upon wetting (Figs. 17, 18) where samples contained thicker fills does suggest the potential for a positive feedback. An initial opening of a fissure would permit more dust penetration, and more dust penetration would then exert additional

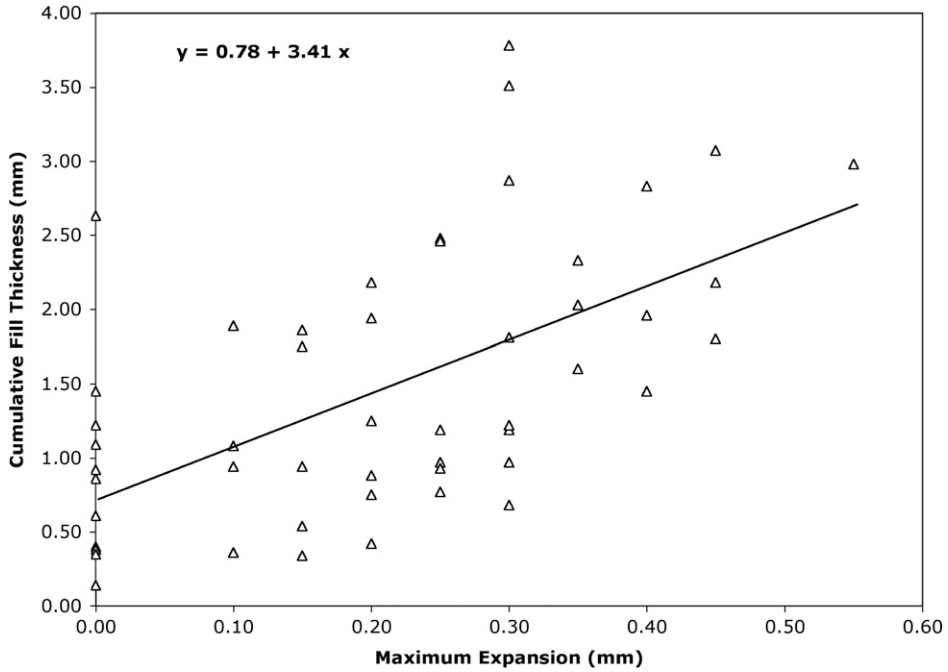

Fig. 17. Results of fracture widening from a single wetting event followed by oven heating, portrayed as a linear regression ($r = 0.56$) of the maximum expansion of fissure fills. Error terms are ± 0.05 on the horizontal and vertical axes.

expansive pressure with wetting events. The implication of this potential positive feedback would be what Ollier (1965) originally suggested — a graduate widening of fissures, allowing more dust penetration that would exert more of a wedging effect.

In the experiment involving just repeated heating and cooling cycles, without wetting, no discernable widening occurred in 64% of the rock chips (Fig. 19). Heating and cooling produced no clear pattern, in those rock chips that did experience widening; the thickness of a fissure fill appeared to play no role in the amount of expansion that did occur. This experiment failed to produce any clear support for Ollier's (1965) original dirt cracking mechanism of insolation-related heating and cooling.

A distinct possibility exists that the shattered condition of the bedrock from homesite construction could exaggerate the observed experimental widening. It is also possible that gravity could similarly exaggerate widening effects, since each rock chip was left 'hanging' while it was exposed to wetting or heating. Any exaggerating effects of shattering and gravity would be seen on all samples. Thus, an additional fifty rock chips were mounted in epoxy and left 'hanging' as control samples for 70 days — or the duration of the longest

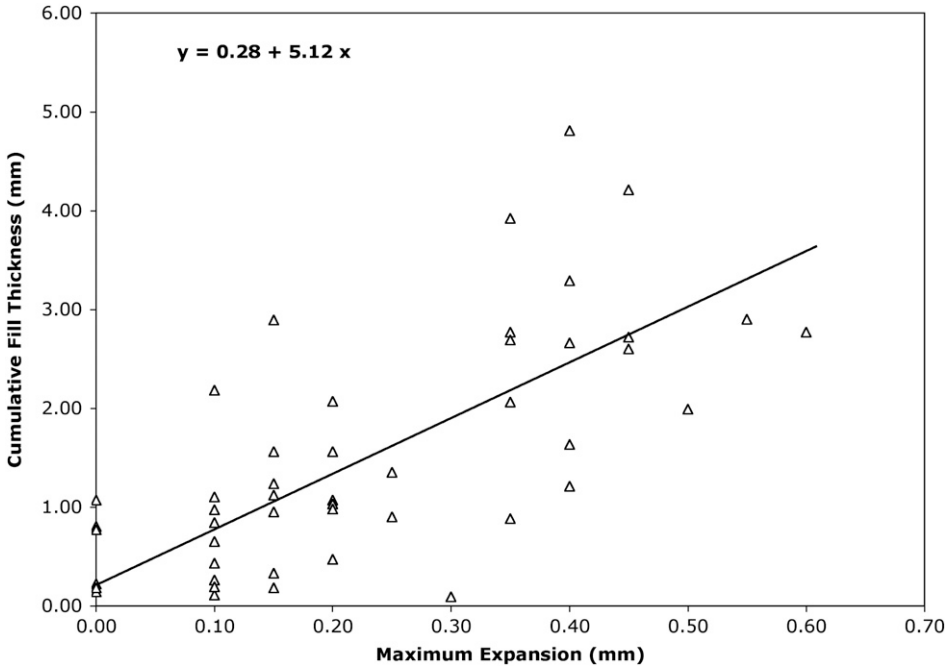

Fig. 18. Results of fracture widening from ten wetting and air drying cycles, portrayed as a linear regression ($r = 0.69$) of the maximum expansion of fissure fills. Error terms are ± 0.05 on the horizontal and vertical axes.

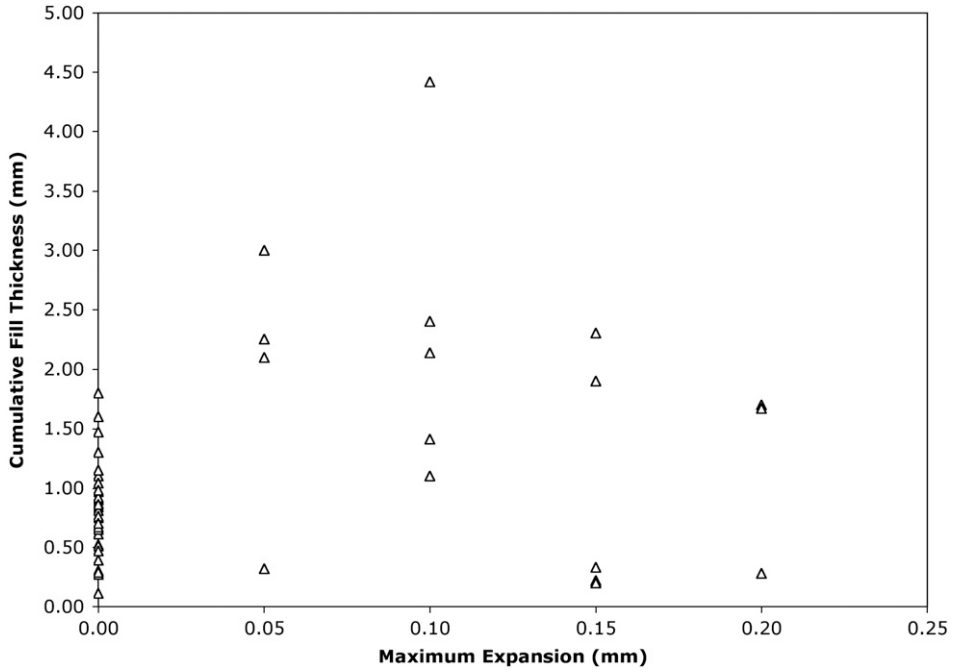

Fig. 19. Results fracture widening from ten heating and cooling cycles, without any wetting, reveal no clear trend in terms of the effect of temperature changes on widening fractures. 64% of the chips showed no measurable widening. Error terms are ± 0.05 on the horizontal and vertical axes.

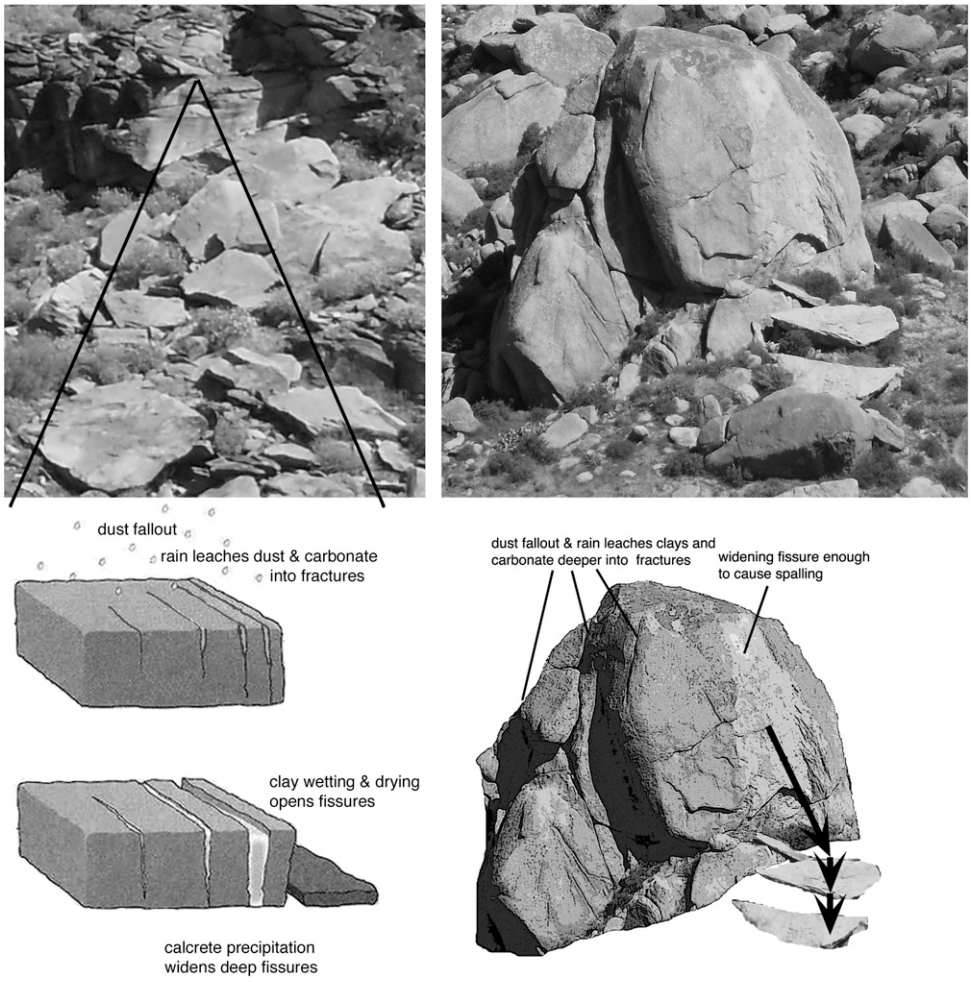

Fig. 20. General process of dirt cracking. The upper left image derives from South Mountain, Phoenix and the upper right from McDowell Mountains, Scottsdale, Arizona. Lower left diagram is intended to illustrate a block a few centimeters thick. The lower right diagram illustrates a core stone over ten meters high.

experiment. Only four of the rock chips showed measurable widening of 0.15, 0.15, 0.25, and 0.30 mm with an error of ±0.05 mm. One possible interpretation of the data portrayed in Fig. 19 could be that some of the widening seen in the heating experiment could simply reflect the effects of shattering and gravity. However, the systematic widening seen in the wetting experiments (Figs. 17, 18) argues for the importance of wetting and drying in fracture widening.

These experiments suffered from additional limitations. They did not employ sophisticated equipment; for example, an atomic force microscope could image expansion processes directly. Furthermore, these experiments were not carried out over long periods of time making repeated measurements in response to cycles heating/cooling or wetting/drying. Still, even with these limitations, gathered data support the hypothesis that wetting fills inside desert rock fractures results in the application of enough force against fracture sides to open fractures.

5. Conclusion

Different processes have been proposed to explain the origins of fractures in desert bedrock and boulders. Insolation effects (Hobbs, 1918; Blackwelder, 1933; Peel, 1974; Warke and Smith, 1998; Paradise, 2005; Moores et al., 2008), moisture changes (Mabbutt, 1977; Camuffo, 1995; Moores et al., 2008), salt weathering (Mortensen, 1933; McGreevy and Smith, 1982; Viles and Goudie, 2007), exfoliation (Blackwelder, 1925), and fire (Dragovich, 1993) all play a role in generating observed fractures. The processes by which fractures undergo enough additional physical weathering to open crevices wide enough to result in detachment are less well understood.

This paper revisits the dirt cracking hypothesis of Ollier (1965), using field observations, light microscopy, electron microscopy, particle size analyses, and laboratory experiments. Ollier's (1965) original notion of dirt cracking involving a positive feedback of crack widening facilitating deeper and deeper penetration of fines is consistent with the evidence gathered in this study. However, there is only one piece of indirect evidence gathered here that supports Ollier's hypothesis that insolation changes results in rock cracking. Observations at South Mountain, Phoenix, suggest that increasing temperatures in late winter and early spring – long after wetting events – could have played a triggering role in a spate of rock spalls observed in 2010. An experiment where rock chips were subjected to heating and cooling cycles, however, did not reveal any expansion effects from fracture fills.

The evidence gathered in this study suggests that dirt cracking appears to be a wedging process started by precipitation of laminar calcrete inside fissures, and then expanded by wetting and drying of expansive clays that exert pressure on fracture sides. The proposed mechanism starts with calcium carbonate precipitating into the narrowest portions of fractures; the precipitation process could play a role in the initial widening of micron-wide fractures. Then, partial dissolution of the carbonate opens enough space to permit the movement of dust, including expansive clays, deeper into the fracture (Fig. 8).

Over time, the clays realign parallel to the fracture walls (Fig. 15); wetting and drying of expansive clays lead to expansive pressures. Widening of the fissure then allows this sequence of carbonate precipitation and dust infiltration to penetrate deeper and deeper into a rock fracture. Eventually, the crack penetrates through enough of the rock and enough force is applied to result in detachment (Fig. 20).

Acknowledgements

This manuscript was supported, in part, by an Arizona State University sabbatical. I thank Arizona State University students for their assistance in the field study of dirt cracking at construction sites. John Dixon, Andrew Plater, and comments of four anonymous reviewers on different iterations of this manuscript greatly improved the paper. I also thank Dave Krinsley for his expertise in electron microscopy.

References

Adelsberger, K.A., Smith, J.R., 2009. Desert pavement development and landscape stability on the Eastern Libyan Plateau, Egypt. Geomorphology 107, 178–194.
Blackwelder, E., 1925. Exfoliation as a phase of rock weathering. Journal of Geology 33, 793–806.
Blackwelder, E., 1933. The insoluation hypothesis of rock weathering. American Journal of Science 26 (152), 97–113.
Bourke, M.C., Viles, H.A., 2007. A Photographic Atlas of Rock Breakdown Features in Geomorphic Environments. Planetary Science Institute, Tucson. 79 pp.
Brazel, A.J., 1989. Dust and climate in the American southwest. Paleoclimatology and Paleometeorology: Modern and Past Patterns of Global Atmospheric Transport. Kluwer Academic Publishers, Dordrecht Dordrecht, pp. 65–96.
Bullard, J.E., Livingston, I., 2009. Dust. In: Parsons, A.J., Abrahams, A.D. (Eds.), Geomorphology of Desert Environments. Springer, New Work, pp. 629–654.
Camuffo, D., 1995. Physical weathering of stones. The Science of the Total Environment 167, 1995.
Certini, G., Corti, G., Ugolini, F.C., DeSiena, C., 2002. Rock weathering promoted by embryonic soils in surface cavities. European Journal of Soil Science 53, 139–146.
Chan, M.A., Yonkee, W.A., Netoff, D.I., Seiler, W.M., Ford, R.L., 2008. Polygonal cracks in bedrock on Earth and Mars: implications for weathering. Icarus 195, 65–71.
Chitale, J.D., 1986. Study of Petrography and Internal Structures in Calcretes of West Texas and New Mexico (Microtextures, Caliche). Ph.D. Dissertation. Thesis Thesis, Texas Tech University, Lubbock, 120 pp.
Clarke, J.D.A., Pain, C.F., 2004. From Utah to Mars: regolith-landform mapping and its application. In: Cocknell, C.C. (Ed.), Martian Expedition Planning. American Astronautical Society and the British Interplanetary Society, London, pp. 131–160.
Cooke, R.U., 1970. Stone pavements in deserts. Annals of the Association of American Geographers 60, 560–577.
Coudé-Gaussen, G., Rognon, P., Federoff, N., 1984. Piegeage de poussières éoliennes dans des fissures de granitoides due Sinai oriental. Compte Rendus de l'Academie des Sciences de Paris II (298), 369–374.
Darmody, R.G., Thorn, C.E., Dixon, J.C., 2008. Differential rock weathering in the 'Valley of the Boulders', Karkevagge Swedish Lapland. Geografiska Annaler A 90A, 201–209.
Dorn, R.I., 2009. Desert rock coatings. In: Parsons, A.J., Abrahams, A. (Eds.), Geomorphology of Desert Environments. Springer, Amsterdam, pp. 153–186.
Dorn, R.I., Whitley, D.S., Cerveny, N.C., Gordon, S.J., Allen, C., Gutbrod, E., 2008. The rock art stability index: a new strategy for maximizing the sustainability of rock art as a heritage resource. Heritage Management 1, 35–70.
Dragovich, D., 1993. Fire-accelerated boulder weathering in the Pilbara, Western-Australia. Zeitschrift für Geomorphologie 37, 295–307.
Engelder, T., 1987. Joints and shear fractures in rock. In: Atkinson, B. (Ed.), Fracture Mechanics of Rock. Academic Press, Orlando, pp. 27–69.
Eppes, M.C., McFadden, L.D., Wegmann, K.W., Scuderi, L.A., 2010. Cracks in desert pavement rocks: further insights into mechanical weathering by directional insolation. Geomorphology 123, 97–108.
Evenari, M., Shanan, L., Tadmor, N., 1982. The Negev. The Challenge of a Desert, Second Edition. Harvard University Press, Cambridge. 437 pp.
Frazier, C.S., Graham, R.C., 2000. Pedogenic transformation of fractured granitic bedrock, southern California. Soil Science Society of America Journal 64, 2057–2069.
Friedman, M., 1975. Fracture in rock. Review of Geophysics and Space Physics 13, 352–358.
Gökceogu, C., Ulusay, R., Sönmez, H., 2000. Factors affecting the durability of selected weak and clay-bearing rocks from Turkey, with particular emphasis on the influence of the number of drying and wetting cycles. Engineering Geology 47, 215–237.
Goudie, A.S., 1978. Dust storms and their geomorphological implications. Journal of Arid Environments 1, 291–310.
Govers, G., Poesen, J., 1998. Field experiments on the transport of rock fragments by animal trampling on scree slopes. Geomorphology 23, 193–203.
Griggs, D.T., 1936. The factor of fatique in rock exfoliation. Journal of Geology 44, 781–796.
Hall, K., 1989. Wind blown particles as weathering agents? An Antarctic example. Geomorphology 2, 405–410.
Haward, M.E., Carstea, D.D., Sayegh, A.H., 1969. Poperties of vermiculites and smectites: expansion and collapse. Clays and Clay Minerals 16, 437–447.
Heilweil, V.M., Solomon, D.K., 2004. Millimeter- to kilometer-scale variations in vadose-zone bedrock solutes: implications for estimating recharge in arid settings. In: Hogan, J.F., Phillips, F.M., Scanlon, B.R. (Eds.), Groundwater Recharge in a Desert Environment: The Southwestern United States. : Water Science and Application Series, Volume 9. American Geophysical Union, Washington D.C, pp. 49–67.
Hobbs, W.H., 1918. The peculiar weathering processes of desert regions with illustrations from Egypt and the Soudan. Michigan Academy of Sciences Annual Report 20, 93–98.
Jimoh, H., 2010. Leading Issues in Geomorphology. Haytee Press and Publishing Company, Ilorin, Nigeria. 51 pp.
Kiernan, K., 1992. Geomorphological evidence for Quaternary climatic change in the low Sino-Burman ranges. Singapore Journal of Tropical Geography 12, 112–123.
Kittrick, J.A., 1969. Quantitative evaluation of the strong-force model for expansion and contraction of vermiculite. Soil Science Society of America Journal 33, 222–225.

Klappa, C.F., 1979. Lichen stromatolites: criterion for subaerial exposure and a mechanism for the formation of laminar calcretes (caliche). Journal of Sedimentary Petrology 49, 387–400.
Knauth, L.P., Brilli, M., Klonowski, S., 2003. Isotope geochemistry of caliche developed on basalt. Geochimica Cosmochimica Acta 67, 185–195.
Mabbutt, J.C., 1977. Desert Landforms. Australian National University Press, Canberra. 340 pp.
Marcus, M.G., Brazel, A.J., 1992. Summer dust storms in the Arizona Desert. In: Janelle, D.G. (Ed.), Geographical Snapshots of North America. Guilford Press, New York, pp. 411–415.
Maricopa-County, 2010. GIS Interactive Maps. http://www.maricopa.gov/Assessor/GIS/javamap.htm. Last Accessed April 10, 2010.
McGreevy, J.P., Smith, B.J., 1982. Salt weathering in hot deserts: observations on the design of simulation experiments. Geografiska Annaler A 64A, 161–170.
Moores, J.E., Pelletier, J.D., Smith, P.H., 2008. Crack propagation by differential insolation on desert surface clasts. Geomorphology 102, 472–481.
Mortensen, H., 1933. Die "Salzprengunt" Und ihre Bedentung für die Regional-klimatische Gliedenung der Wüsten. Petermanns Geographische Mitteilungen 79, 130–135.
Ollier, C.D., 1965. Dirt cracking — a type of insolation weathering. Australian Journal of Science 27, 236–237.
Ollier, C.D., 1969. Weathering. Oliver & Boyd, Edinburgh. 304 pp.
Ollier, C.D., 1978. Inselbergs of the Namib Desert, processes and history. Zeitschrift fur Geomorphologie Supplementband 31, 161–176.
Pain, C.F., 1985. Cordilleran metamorphic core complexes in Arizona: a contribution from geomorphology. Geology 13, 871–874.
Paradise, T.R., 2005. Petra revisited: an examination of sandstone weathering research in Petra, Jordan. Geological Society of America Special Paper 390, 39–49.
Peel, R.F., 1974. Insolation weathering: some measurements of diurnal temperature changes in exposed rocks in the Tibesti region, central Sahara. Zeitschrift für Geomorphologie Supplement Band 21, 19–28.
Péwé, T.L., Péwé, R.H., Journaux, A., Slatt, R.M., 1981. Desert dust: characteristics and rates of deposition in central Arizona. Geological Society of America Special Paper 186, 169–190.
Reynolds, S.J., 1985. Geology of the South Mountains, central Arizona. Arizona Bureau of Geology and Mineral Technology Bulletin 195, 1–61.
Richards, S.M., Reynolds, S.J., Spencer, J.E., Pearthree, P.A., 2000. Geologic map of Arizona. Arizona Geological Survey Map M-35, 1 sheet, scale 1:1,000,000.
Rockrock, E.P., 1925. On the force of crystallization of calcite. Journal of Geology 33, 80–83.
Schlesinger, W.H., 1985. The formation of caliche in soils of the Mojave Desert, California. Geochimica et Cosmochimica Acta 49, 57–66.
Smith, B.J., 1988. Weathering of superficial limestone debris in a hot desert environment. Geomorphology 1, 355–367.
Smith, B.J., 1994. Weathering processes and forms. In: Abrahams, A.D., Parsons, A.J. (Eds.), Geomorphology of Desert Environments. Chapman & Hall, London, pp. 39–63.
Smith, B.J., 2009. Weathering processes and forms, In: Parsons, A.J., Abrahams, A.D. (Eds.), Geomorphology of Desert Environments, 2nd edition. Springer, Amsterdam, pp. 69–100.
Smith, B.J., Srinivasan, S., Gomez-Heras, M., Basheer, P.A.M., Viles, H.A., 2011. Near-surface temperature cycling of stone and its implications for scales of surface deterioration. Geomorphology 130, 76–82.
Thoma, S.G., Gallegos, D.P., Smith, D.M., 1992. Impact of fracture coatings on fracture/matrix flow interactions in unsaturated, porous media. Water Resources Research 28, 1357–1367.
Vaniman, D.T., Whelan, 1994. Inferences of paleoenvironment from petrographic, chemical and stable-isotope studies of calcretes and fracture calcites. Report Number: LA-UR-94-640 CONF-940553-13. In: Sanders, T.L. (Ed.), High Level Radioactive Waste Management 1994. : Proceedings of the Fifth Annual International Conference, Las Vegas, Nevada, May 22–26, 1994. American Society of Civil Engineers, New York, pp. 2730–2737.
Viles, H.A., 2005. Microclimate and weathering in the central Namib Desert, Namibia. Geomorphology 67, 189–209.
Viles, H.A., Goudie, A.S., 2007. Rapid salt weathering in the coastal Namib desert: implications for landscape development. Geomorphology 85, 49–62.
Villa, N., Dorn, R.I., Clark, J., 1995. Fine material in rock fractures: aeolian dust or weathering? In: Tchakerian, V. (Ed.), Desert Aeolian Processes. Chapman & Hall, London, pp. 219–231.
Warke, P.A., 2007. Complex weathering in drylands: implications of 'stress' history for rock debris breakdown and sediment release. Geomorphology 85, 30–48.
Warke, P.A., Smith, B.J., 1998. Effects of direct and indirect heating on the validity of rock weathering simulation studies and durability tests. Geomorphology 22, 347–357.
Watanabe, T., Sato, T., 1988. Expansion characteristics of montmorillonite and sapronite under various relative humidity conditions. Clay Science 7, 129–138.
Williams, R., Robinson, D., 1989. Origin and distribution of polygonal cracking of rock surfaces. Geografiska Annaler 71A, 145–159.
Wright, V.P., 1989. Terrestrial stromatolites and laminar calcretes — a review. Sedimentary Geology 65, 1–13.
Young, R.G., 1964. Fracturing of sandstone cobbles in caliche cemented terrace gravels. Journal of Sedimentary Petrology 34, 886–889.